Electrical properties of silicon nitride films prepared by electron cyclotron resonance assisted sputter deposition

K. Deenamma Vargheese and G. Mohan Rao[a)]
Department of Instrumentation, Indian Institute of Science, Bangalore 560012, India

Silicon nitride films have been deposited using electron cyclotron resonance (ECR) plasma-assisted rf sputter deposition. Variation in composition and electrical properties of the deposited films has been studied. Films with specific resistivity of 10^{13} Ω cm and a dielectric constant of 7 have been obtained at a ECR power of 100 W (corresponding to an ion flux of 1×10^{10} cm^{-3}). These films exhibited minimum interface density of 2×10^{10} $\mathrm{eV}^{-1}\,\mathrm{cm}^{-2}$ and have a critical field of 5 MV/cm. Detailed electrical characterization of the films has been carried out to study the variation of interface density with ECR power and to identify the conduction mechanism.

I. INTRODUCTION

Silicon nitride (Si_3N_4) is an important material in microelectronics due to its high resistivity, higher dielectric constant compared to silicon dioxide, mechanical strength, and chemical inertness.[1–3] It is used as a gate insulator in thin film transistors that are in flat panel displays. It is also used in nonvolatile memory devices because of its trapping ability. It can be applied as an oxidation mask and diffusion barrier in integrated circuit technology. Si_3N_4 films are mainly prepared by chemical vapor deposition (CVD)[4,5] and plasma enhanced chemical vapor deposition (PECVD).[6–11] Even though chemical vapor deposition is widely used for the deposition of Si_3N_4 films, the main disadvantages of this technique are the incorporation of hydrogen in the films and high substrate temperature. The entrapped hydrogen in the films can deteriorate the properties of Si_3N_4, and the high substrate temperature is not generally desired in microelectronic applications. Reactive sputtering[11,12] at low substrate temperature can provide Si_3N_4 films with extremely low hydrogen content. In addition, the properties of the films can be tailored with ion assistance. But the main problem encountered in ion-assisted deposition of silicon nitride films is that the ion bombardment during the film growth induces many defects in the film which in turn degrade the electrical properties.[13] These defects are due to the higher energy and flux of the ions bombarding the growing film. Thus a flexibility in controlling the flux and energy of the ions will facilitate in the growth of thin films of desired properties. In this respect electron cyclotron resonance (ECR) plasma, which is commonly used for PECVD, provides an excellent choice. The low energy high dense plasma which is produced by an ECR ion source can be used for the ion-assisted deposition of thin films. The high reactivity of the gas species and low pressure operation is an added advantage. To the best of our knowledge, there are not many reports on the successful use of ion bombardment to deposit good quality Si_3N_4 films. We have been able to deposit stoichiometric silicon nitride films using ECR plasma-assisted sputter deposition.[14] In this article we discuss in detail the electrical properties of silicon nitride films prepared by ECR assisted deposition. The electrical properties are studied using capacitance–voltage ($C-V$) and current–voltage ($I-V$) measurements. The effect of ion assistance on the interface state density, resistivity, and critical field is discussed.

a)Electronic mail: gmrao@isu.iisc.ernet.in

II. EXPERIMENT

In the present study we have used a ECR plasma-assisted sputter deposition system developed in our laboratory for the deposition of SiN_x films.The schematic of the ECR sputtering system used for the deposition of silicon nitride films is shown in Fig. 1. A 2 kW water-cooled cw magnetron is used as the microwave source. This is connected to the ECR source chamber through an isolator, directional coupler, tuner, and a mode convertor. The isolator provides the necessary protection for the microwave source from the reflected power. The forward and reflected power are measured using the directional coupler, and the tuner is used for the impedance matching. This microwave circuitry is connected to the cylindrical source chamber using a mode convertor. Two electromagnetic coils surrounding the water-cooled source chamber produce the ECR resonance zone and confine the electrons inside the source chamber. The microwaves enter the source chamber through a quartz window. The source chamber is provided with a quartz liner to avoid contamination from the wall of the source chamber. More details about the ECR plasma analysis have been discussed in our earlier publication.[14]

SiN_x films are prepared using a rf powered magnetron sputter cathode which is fixed with a 100 mm silicon target. Single crystal p-type Si (100) substrates have been mounted at a distance of 100 mm orthogonally from the target on a heated platform kept at 350 °C. This arrangement facilitates direct bombardment of ECR plasma on the growing film. The Si substrates were cleaned by standard RCA cleaning. All the films have been deposited with a rf power of 220 W, nitrogen partial pressure of 2.5×10^{-4} mbar, and a total pres-

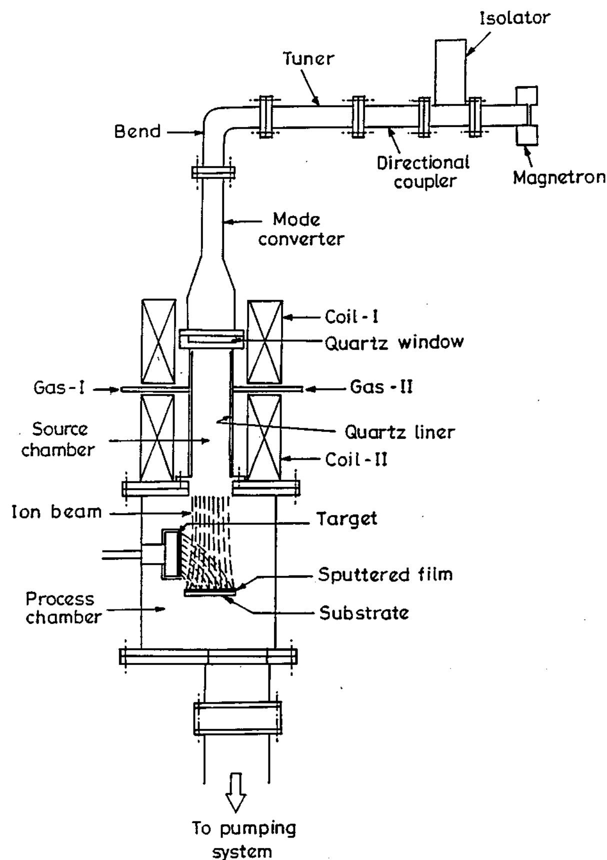

FIG. 1. Schematic of the ECR system.

sure of 1.5×10^{-3} mbar. The gas flow was maintained using a Teledyne-Hasting mass flow controller. Films with a thickness of 170 nm are prepared with different ECR powers to vary the ion flux bombardment of the substrate during the film growth. The power was varied from 0 to 250 W. The ion density near the substrate was measured using a Langmuir probe without the target plasma. The variation of the ion flux near substrate with ECR power is shown in Fig. 2. It varied from 8×10^{9} to 2.4×10^{10} cm^{-3} as the power was increased

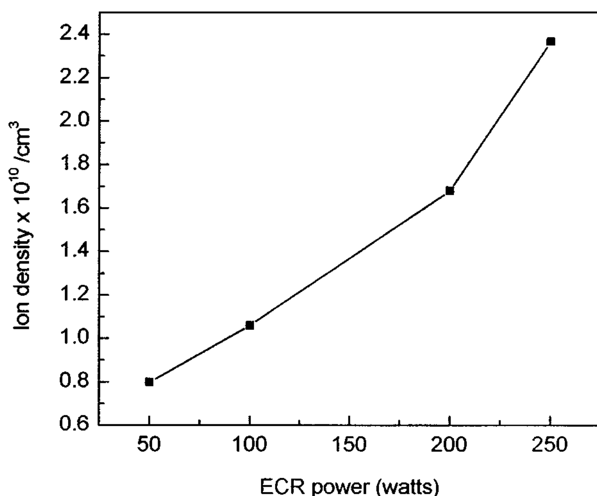

FIG. 2. Variation of ion flux with ECR power near the substrate.

TABLE I. Composition of silicon nitride films as measured by AES.

Sample No.	ECR power (W)	Composition (Si/N)
1	0	1
2	50	0.82
3	100	0.73
4	200	0.68
5	250	0.85

from 50 to 250 W. The target substrate distance was maintained at 100 mm so as to decouple the rf plasma and the ECR ion beam. The samples prepared under different ECR powers are designated as shown in the Table I. Composition analysis of these samples was done using Auger electron spectroscopy (AES). To carry out the electrical measurements in metal-insulator-semiconductor (MIS) configuration, aluminum electrodes (6.7×10^{-3} cm^2) were deposited on silicon nitride using a shadow mask. Aluminum was deposited on the back of the *p*-type silicon substrate to provide the ohmic contact. The $C-V$ measurements were carried out using a Kiethly $C-V$ analyzer (model 590) meter at a frequency of 1 MHz. The measurements were done at room temperature. A programmable Kiethly electrometer (model 6517) was used to measure the $I-V$ characteristics. The voltage was scanned at a rate of 70 mV/s.

III. RESULTS AND DISCUSSION

A. Composition analysis

The composition of the films analyzed using AES is shown in Table I. It shows that the films prepared with zero ECR power are silicon rich. The amount of nitrogen in the sample increases as the ECR power is increased. This increase in nitrogen content in the film is due to the higher reactivity of ECR plasma. At 100 W the ratio of Si/N is about 0.73 as shown by the AES analysis. This corresponds to nearly stoichiometric Si_3N_4. Films deposited with higher ECR power again showed an increase in silicon content. This can be attributed to the resputtering of nitrogen due to bombardment of higher ion flux. Though the films deposited without ECR assistance and high power ECR plasma are silicon rich, the nature of the bonding in these films is different. X-ray photoemission studies carried out on the samples showed this difference. The Si $2p$ peak for sample 1 is at 101.6 eV, and for sample 5 is at 102.2 eV, which corresponds to Si_3N_4. The shift of 0.6 eV indicates a lesser number of Si–N bonds[15] in sample 1 compared to sample 5. This means that the chemical environment of Si in sample 1 differs from sample 5. The composition analysis clearly shows that for given conditions like sputtering pressure, target-substrate distance, and substrate temperature the film composition depends on the ion flux.

B. Electrical properties

1. Capacitance–voltage characteristics

The capacitance–voltage ($C-V$) characteristics of samples 1, 3, and 5 are given in Figs. 3(a)–3(c). The figures

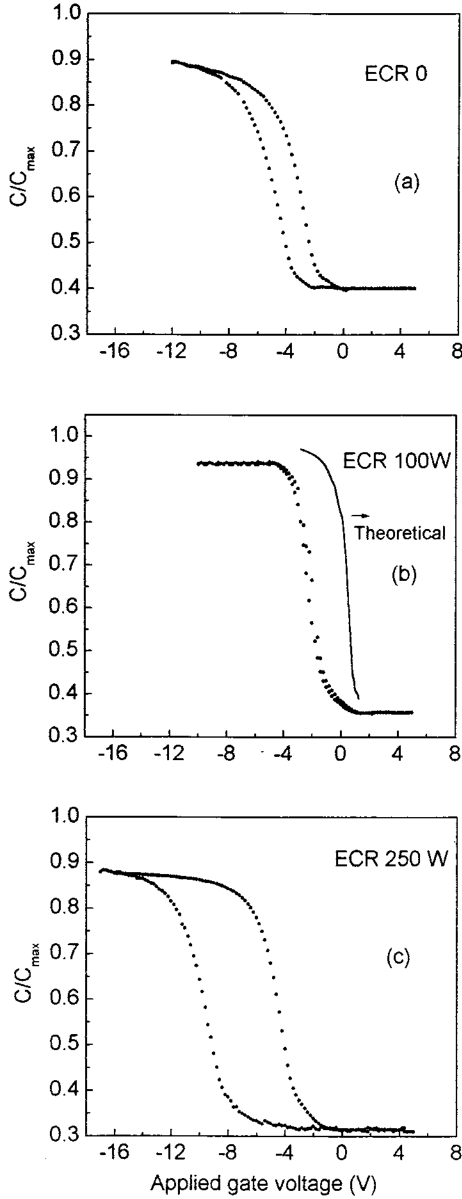

FIG. 3. Capacitance–voltage characteristics of samples. (a) Sample 1, (b) sample 3, and (c) sample 5.

clearly show the accumulation, depletion, and inversion regions for the MIS capacitor. The $C-V$ characteristics of the samples exhibit a considerable change in terms of flatband voltage and hysteresis width with ECR power. The capacitance–voltage measurements were used to study the variation of dielectric constant and interface state density. The dielectric constant, hysteresis width, and interface density obtained from the $C-V$ characteristics are shown in Table II. As seen from the table, the dielectric constant is slightly high for sample 1. The dielectric constant for sample 3 is 7 and is in agreement with the reported value for Si_3N_4 films. The higher value of the dielectric constant for sample 1 could be due to the higher silicon content present in these films as shown by the composition analysis. The forward and reverse trace of the $C-V$ curve showed anticlockwise hysteresis which indicates hole injection into silicon nitride film.[16] As shown in Figs. 3(a)–3(c) and Table II, the hysteresis width for the samples reduces as the ECR power is increased and reaches a minimum of around 0.5 V for sample 3. The negative shift and the hysteresis width for samples 1 and 5 were much higher compared to sample 3. The high value of hysteresis width and flatband shift can be attributed to the positive traps present in SiN film and the interface. The nature of the defects in silicon-rich, stoichiometric and nitrogen-rich SiN_x films was studied in detail.[17,18] The behavior of silicon-rich films was described with a model of multiple dangling bond configuration. In stoichiometric and nitrogen-rich films the defects are mainly constituted by silicon dangling bonds ($.Si{\equiv}N_3$). These traps are amphoteric in nature, i.e., these defects can trap positive and negative charges. Thus the large negative flatband voltage shift in the present study indicates the presence of silicon dangling bonds. The positive trap density calculated from the negative shift for sample 3 is 5×10^{11} cm^{-2}. For samples 1 and 5 it is 2×10^{12} and 3×10^{12} cm^{-2}, respectively.

The interface state density has been calculated using Terman's analysis[19] for high frequency $C-V$ measurements. This analysis is based on the comparison of the high frequency measured curve and the theoretical curve. In Fig. 2 the solid line corresponds to the theoretical curve. Figure 4 shows the interface density distribution in the forbidden gap. The interface density at the flatband voltage is determined using Lehovich's[20] method and is compared with the value obtained using Terman's method. The interface density for sample 3 is much lower compared to samples 1 and 5. The higher value of interface density for samples 1 and 5 compared to sample 3 can be due to the presence of silicon dangling bonds at the interface.

TABLE II. Dielectric constant, hysteresis width, flatband shift, and interface density (D_i) obtained from $C-V$ measurements.

Sample	Dielectric constant	Hysteresis width (V)	Flatband shift (V)	D_i at flatband (Terman's method) (eV^{-1} cm^{-2})	D_i at flatband (Lehovich method) (eV^{-1} cm^{-2})
1	7.9	2.2	7	2×10^{11}	2.7×10^{12}
2	6.7	1.1	7	2×10^{11}	2^{12}
3	6.83	0.34	2	2×10^{10}	2×10^{11}
4	6.3	0.75	3.6	5×10^{10}	3.6^{11}
5	6.2	5.1	11.9	3×10^{11}	5^{12}

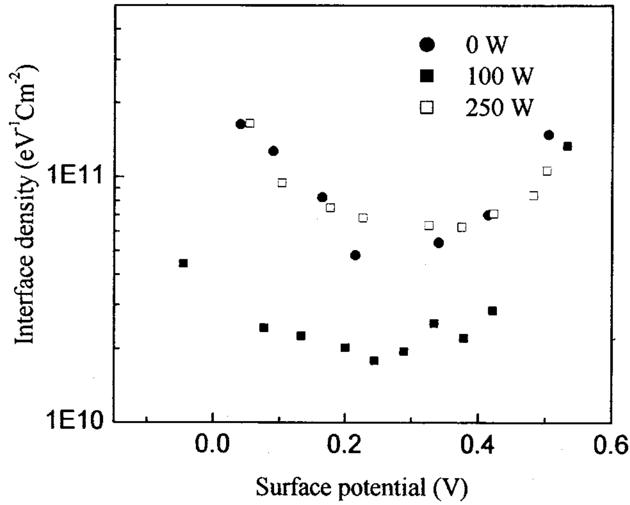

FIG. 4. Variation of interface state density with surface potential.

According to Lehovich the interface density (D_i) at the flatband is given by

$$D_i = \frac{(C_0 - C)C}{3qkT\partial C/\partial V} - \frac{C_0^2}{C_0 - C}\frac{1}{q}, \tag{1}$$

where C_0 is the silicon nitride capacitance, C is the measured capacitance at flatband voltage, $\partial C/\partial V$ is the slope of the $C-V$ curve at flat band, q is the electron charge, T is the temperature of measurements, and k is Boltzmann's constant. The values of interface density calculated from both methods are shown in Table II. Both the methods show that the interface density is minimum for the films prepared at 100 W of ECR power. Another feature is that the interface density calculated by Terman's analysis is one order less compared to that calculated by Lehovich's method. Landheer *et al.*[16] have calculated the interface density of PECVD SiN_x films using Terman's method and quasistatic measurements. Also, in this case Terman's method gave less interface density compared to the quasistatic measurements. The minimum interface density obtained in the present study is comparable to the reported value of interface density for PECVD films.[21] Hugon[21] *et al.* reported a value of 6×10^{10} cm^{-2}eV^{-1} for PECVD SiN_x films from high frequency and quasistatic measurements. The minimum capacitance obtained in the $C-V$ measurements for sample 3 has been used to calculate the doping concentration of the p-type substrate used in the study. The value obtained deviates slightly from the manufacturer's data. This deviation can be due to the presence of interface states as discussed above. The $C-V$ analysis shows that sample 3 which is prepared at 100 W of ECR power has the minimum trap density and interface density. In conclusion, the $C-V$ measurements of the samples prepared at different ECR powers reveal that with optimum ECR assistance, Si_3N_4 films with low interface density and hysteresis can be produced. In the present study this optimum ECR assistance corresponds to an ion flux of 1×10^{10} cm^{-3}.

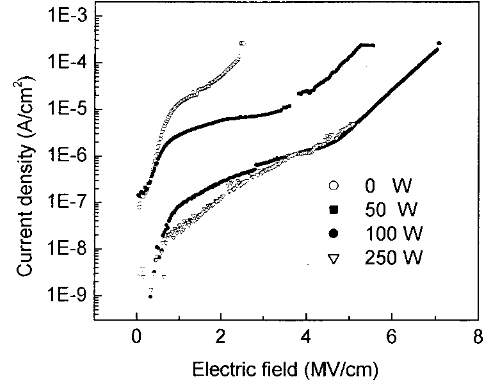

FIG. 5. $I-V$ characteristics of a sample prepared at different ECR power.

2. I–V characteristics

To study the insulating properties of SiN_x films, the leakage current measurements of the samples were carried out. The measurements were done with the sample bias in the accumulation region. Later measurements were carried out by changing the polarity of the electrodes. There is no significant change in the leakage current. This clearly indicates that the conduction mechanism in these films is not electrode dependent but is controlled by the bulk of the film.[22] Figure 5 shows the $I-V$ characteristics of the samples. The $I-V$ characteristics show three regions, i.e., low field, intermediate field, and high field regions, with different slopes. The resistivity and the critical fields obtained from the $I-V$ measurements are shown in Fig. 6. The critical field is defined as the field where the current density is 1 μA/cm^2. Samples 1 and 2 have a resistivity of 10^{12} Ω cm and the critical field is less than 2 MV/cm. But for sample 3, the resistivity is 10^{13} Ω cm and the critical field is 5 MV/cm. The resistivity value is slightly lower compared to the reported values for Si_3N_4 on p-type silicon by PECVD. Resistivity of 10^{16} Ω cm is reported for Si_3N_4 on n-type silicon.[21] Even though the posi-

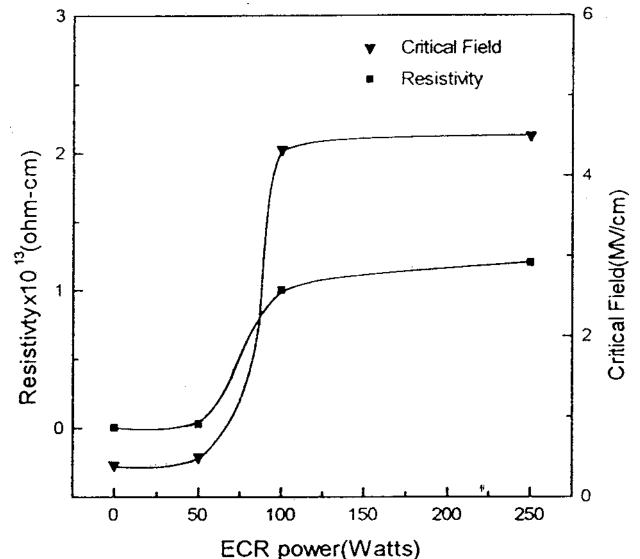

FIG. 6. Variation of resistivity and critical field with ECR power.

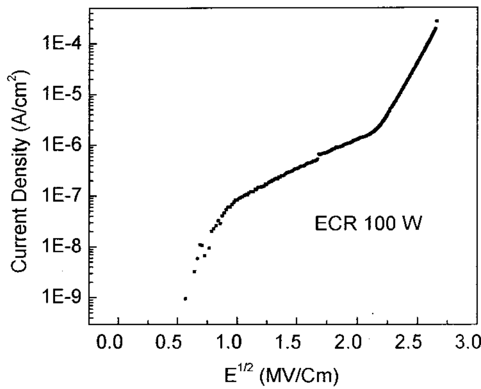

FIG. 7. J vs $E^{1/2}$ plot of sample 3.

tive trap density calculated from $C-V$ measurement for sample 5 is much higher than sample 3, the leakage current and critical field is comparable to that of sample 3. The low resistivity of Si_3N_4 on p-type is due to the hole injection from p-type silicon to the insulator. According to Yun[23] the hole trap density and electron trap density can be considered equal. In Si_3N_4 the hole levels are shallower than the electron levels, so the holes are more easily detrapped and are more mobile.[23,24] This higher mobility can be attributed to the lower resistivity of Si_3N_4 on p-type substrates. The linearity of the current density versus square root of the electrical field (Fig. 7) in the high field region indicates that the conduction mechanism in ECR assisted Si_3N_4 films is either Poole and Frenkel or Schottky emission. The symmetry of the $I-V$ characteristics, irrespective of the polarity of the electrodes, indicates that the current transport in Si_3N_4 film is bulk controlled. Thus the leakage current in the high field region can be explained using the Poole and Frenkel conduction mechanism. According to the Poole and Frenkel emission mechanism,

$$J = CE \exp^{[-q(\phi_b - \sqrt{qE/\pi\epsilon_d\epsilon_0})/kT]}, \tag{2}$$

where J is the current density, C is a constant determined by the trap density in the film, ϕ_b is the Poole and Frenkel barrier height, and ϵ_0 and ϵ_d are the free space and dynamic dielectric constants. ϵ_d can be obtained from the slope of $\ln J$ versus $E^{1/2}$. The dynamic dielectric constant obtained from the slope of $\ln(J)-E^{1/2}$ in the high field region for sample 3 is 7. The dielectric constant obtained from the $C-V$ measurements is 7. The optical dielectric constant obtained from the UV-Visible transmission spectra is 3.9. For the Poole and Frenkel conduction mechanism the dynamic dielectric constant should be between 7 and 3.9. The value obtained for the dynamic dielectric constant from $\ln(J)-E^{1/2}$ supports the Poole–Frenkel conduction mechanism in ECR assisted SiN_x films.

IV. CONCLUSIONS

A detailed study on the electrical properties of SiN_x films prepared by ECR assisted sputter deposition has been carried out. Composition analysis using AES shows that stoichiometric Si_3N_4 films can be deposited with a ECR power of 100 W which corresponds to an ion flux of 1×10^{10} cm^{-3} on the substrate. Films grown without ECR assistance and with higher ECR power (250 W) are silicon rich. The films prepared with 100 W ECR power showed a dielectric constant of 7, critical field of 5 MV/cm, and high resistivity of 10^{13} Ω cm. These films are of device quality with a minimum interface density of 2×10^{10} eV^{-1} $^{-2}$. In conclusion, we have shown that using ECR plasma assisted sputter deposition, device quality Si_3N_4 films could be deposited.

ACKNOWLEDGMENTS

The authors thank Dr. Reddy and M. Ramachandran for their help in $C-V$ measurements and Dr. Sangunni and Asha Bhat for the $I-V$ measurements.

[1]T. P. Ma, IEEE Trans. Electron Devices **45**, 680 (1998).
[2]N. Lustig and J. Kanicki, J. Appl. Phys. **65**, 3951 (1989).
[3]A. K. Sinha, H. J. Levinstein, T. E. Smith, G. Quintana, and S. E. Haszko, J. Electrochem. Soc. **125**, 601 (1978).
[4]S. Trolier-McKinstry, H. Hu, and A. H. Carim, J. Electrochem. Soc. **141**, 2483 (1994).
[5]S. V. Deshpande, E. Gulari, S. W. Brown, and S. C. Rand, J. Appl. Phys. **77**, 6534 (1995).
[6]D. G. Park, M. Tao, D. Li, A. E. Botchkarev, Z. Fan, Z. Wang, S. N. Mohammad, A. Rockett, J. R. Abelson, H. Morkoc, A. R. Heyd, and S. A. Alterovitz, J. Vac. Sci. Technol. B **14**, 2674 (1996).
[7]S. Sitbon, M. C. Hugon, B. Agius, F. Abel, J. L. Courant, and M. Puech, J. Vac. Sci. Technol. A **13**, 2900 (1995).
[8]M. Maeda and K. Ikeda, J. Appl. Phys. **83**, 3865 (1998).
[9]C. Doughty, D. C. Knick, J. B. Bailey, and J. E. Spencer, J. Vac. Sci. Technol. A **17**, 2612 (1999).
[10]D. Landheer, K. Rajesh, D. Masson, J. E. Huise, G. I. Sproule, and T. Quance, J. Vac. Sci. Technol. A **16**, 2931 (1998).
[11]J. H. Kim and K. W. Chung, J. Appl. Phys. **83**, 5831 (1998).
[12]S. K. Ray, S. Das, C. K. Maiti, S. K. Lahiri, and N. B. Chakraborti, J. Appl. Phys. **75**, 8145 (1994).
[13]M. F. Lambrinos, R. Valizadeh, and J. S. Colligon, J. Vac. Sci. Technol. B **16**, 589 (1998).
[14]K. Deenamma Vargheese and G. Mohan Rao, Rev. Sci. Instrum. **71**, 467 (2000).
[15]R. Karcher, L. Ley, and R. L. Johnson, Phys. Rev. B **30**, 1896 (1984).
[16]D. Landheer, Z. H. Lu, J. M. Baribeau, L. J. Huang, and W. M. Lau, J. Electron. Mater. **23**, 943 (1994).
[17]D. Jousse, J. Kanicki, and J. H. Stathis, Appl. Surf. Sci. **39**, 412 (1989).
[18]W. L. Warren, J. Kanicki, F. C. Rong, and E. H. Poindexter, J. Electrochem. Soc. **139**, 880 (1992).
[19]L. M. Terman, Solid-State Electron. **5**, 285 (1962).
[20]K. Lehovech, Solid-State Electron. **11**, 135 (1968).
[21]M. C. Hugon, F. Delmotte, and B. Agius, J. Vac. Sci. Technol. A **15**, 3143 (1997).
[22]S. M. Sze, J. Appl. Phys. **38**, 2951 (1967).
[23]B. H. Yun, Appl. Phys. Lett. **27**, 256 (1975).
[24]P. C. Arnett and Z. A. Weinberg, IEEE Trans. Electron Devices **ED-25**, 1074 (1978).